Published in final edited form as:
Nature. 2009 April 2; 458(7238): 655–659. doi:10.1038/nature07763.

Clustering of IP_3 receptors by IP_3 retunes their regulation by IP_3 and Ca^{2+}

Taufiq-Ur-Rahman[1], **Alexander Skupin**[2], **Martin Falcke**[2,3], and **Colin W. Taylor**[1]

[1]Department of Pharmacology, Tennis Court Road, Cambridge, CB2 1PD, UK

[2]Mathematical Cell Physiology, Max Delbrück Centre for Molecular Medicine, Robert Rössle Str. 10, 13092 Berlin, Germany

[3]Helmoholtz Centre Berlin for Materials and Energy, Glienicker Str. 100, 14109 Berlin, Germany

Abstract

The versatility of Ca^{2+} signals derives from their spatio-temporal organization1,2. For Ca^{2+} signals initiated by inositol trisphosphate (IP_3) this requires local interactions between IP_3 receptors (IP_3R)3,4 mediated by their rapid stimulation and slower inhibition4 by cytosolic Ca^{2+}. This allows hierarchical recruitment of Ca^{2+} release events as the IP_3 concentration increases5. Single IP_3R respond first, then clustered IP_3R open together giving a local Ca^{2+} puff, and as puffs become more frequent they ignite regenerative Ca^{2+} waves1,5-9. We demonstrate, using nuclear patch-clamp recording10, that IP_3R are initially randomly distributed with an estimated separation of ~1 μm. Low concentrations of IP_3 cause IP_3R to aggregate rapidly and reversibly into small clusters of ~4 closely associated IP_3R. At resting cytosolic [Ca^{2+}], clustered IP_3R open independently, but with lower open probability (P_o), shorter open time, and lesser IP_3 sensitivity than lone IP_3R. Increasing cytosolic [Ca^{2+}] reverses the inhibition caused by clustering, IP_3R gating becomes coupled, and the duration of multiple openings is prolonged. Clustering both exposes IP_3R to local Ca^{2+} rises and increases the effects of Ca^{2+}. Dynamic regulation of clustering by IP_3 tunes IP_3R sensitivity to IP_3 and Ca^{2+}, facilitating hierarchical recruitment of the elementary events that underlie all IP_3-evoked Ca^{2+} signals3,5.

IP_3-activated currents recorded from patches excised from the outer nuclear envelope of DT40 cells10 expressing rat IP_3R3 are entirely due to IP_3R3 (Fig. 1). With 10 μM IP_3 in the pipette solution (PS) the single channel open probability (P_o) was 0.44 ± 0.05 (n = 6) and the mean open time (τ_o) was 11.9 ± 1.6 ms. The distribution of closed times (τ_c) had two components (Fig. 1d). Recordings in the on-nucleus configuration confirmed these results (not shown). The results are consistent with the gating scheme shown in Figure 1d (see Supplementary Methods).

The number of channels within a patch (1.34 ± 0.13, n = 109) can be estimated reliably from the largest multiple of simultaneous openings to the unitary current level (Fig. 1e, Methods). The distribution of IP_3R in a patch is random: it is not significantly different from a Poisson distribution (χ^2, $p>0.05$; Fig. 1f, Supplementary Table 1). Others suggested that IP_3R are clustered in the nuclear envelope11,12, but it seems likely that in making repeated recordings from the same nucleus they stimulated nuclei with IP_3 before recording and thereby caused IP_3R clustering (see below).

Channel activity (P_o, Fig. 2a-c), but not the number of active IP_3R (Fig. 2d), increased with IP_3 concentration (EC_{50} = 1.38 ± 0.03 μM for patches with one IP_3R). There was more than

Author information Correspondence and requests for materials should be addressed to C.W.T. (cwt1000@cam.ac.uk)..

Europe PMC Funders Author Manuscripts

one IP_3R in 57% of active patches, and each opened to the same γ (Fig. 1e, 2a), but NP_o (the overall channel activity) was less than expected from the summed behaviour of lone IP_3R (Fig. 2e). For multi-IP_3R patches, the sensitivity to IP_3 of NP_o was also significantly reduced (EC_{50} = 2.47 ± 0.25 μM for patches with 3 IP_3R, Fig. 2c, Supplementary Table 2). Do IP_3R behave independently in such multi-IP_3R patches or do they interact, like some ryanodine receptors13,14? For each of the four states in patches with three IP_3R (closed and 1, 2 or 3 simultaneously open IP_3R), P_o predicted from the binomial distribution matched the observed P_o (Fig. 2f, Methods). Similar results were obtained for patches with different numbers of IP_3R and for type 1 IP_3R (Supplementary Figs 1, 2). At resting cytosolic [Ca^{2+}], therefore, each IP_3R within a multi-IP_3R patch behaves identically and opens independently.

How can randomly distributed IP_3R that open independently behave with such uniformity, and yet so differently from lone IP_3R, when a patch fortuitously contains several IP_3R? Recordings from *Xenopus* nuclei also suggest that heterogenous behaviour of lone IP_3R becomes more uniform when patches contain several IP_3R15. We suggest that IP_3 causes IP_3R to cluster16 and that clustered IP_3R are less active. To test this hypothesis, nuclei were bathed in IP_3 (10 μM, 2 min) before forming seals for patch-clamp recording. In these paired experiments, the mean number of IP_3R per patch was unaffected by IP_3-pre-treatment (Supplementary Table 1), confirming that IP_3 neither inactivated IP_3R nor affected the area of membrane trapped beneath the patch. But the distributions of IP_3R were very different before and after IP_3 treatment (Fig. 3a). In naïve nuclei IP_3R were randomly distributed (Fig. 3b), but their distribution after IP_3-pre-treatment differed significantly from the Poisson distribution ($p<0.05$): many patches had no IP_3R, single IP_3R were under-represented, and several patches had unusually large numbers of IP_3R (Fig. 3c). This clustering of IP_3R fully reversed within 8-10 min of removing IP_3 (Fig. 3a, d). P_o of lone IP_3R from naïve nuclei (0.44 ± 0.05, n = 6) was indistinguishable from P_o of the only lone IP_3R caught within a patch after IP_3 pre-treatment (0.41). P_o for each IP_3R within a cluster was also indistinguishable for recordings from naïve (0.24 ± 0.01, n = 18) and IP_3-pre-treated nuclei (0.25 ± 0.01, n = 18). Furthermore, there was no decrease in P_o during recordings that outlasted the IP_3 pre-treatment (Supplementary Fig. 3). We conclude that clustering, rather than IP_3 *per se*, decreases P_o.

The decrease in P_o as IP_3R cluster is identical whether clustering is evoked by application of IP_3 to an isolated patch (Fig. 2e, h) or the entire nucleus (Fig. 3e). Both reduce P_o to ~54% that of lone IP_3R. The latter condition better replicates the situation *in vivo*, confirming that results with isolated patches (Figs 1, 2) faithfully report the behaviour of IP_3R roaming freely within the nuclear envelope. The effect of cluster size on P_o indicates that pairing of IP_3R is sufficient to cause the maximal decrease in P_o. Additional IP_3R can join a cluster, and their activity is attenuated, but IP_3R within larger clusters are no more inhibited than pairs of IP_3R (Figs 2g, h, Supplementary Table 2). IP_3R associate with actin4 and microtubules17, but neither is required for clustering-evoked changes in P_o (Supplementary Fig. 4).

To examine the effects of clustering on IP_3R gating, we compared mean open time (τ_o, Supplementary Information) of lone IP_3R with τ_o for single channel openings from patches with several (N) IP_3R (blue line in Fig. 3f). These τ_o should be similar if lone and grouped IP_3R behave identically. For multi-IP_3R patches, we also measured the duration of events in which all IP_3R were simultaneously open ($\tau_{o,N}$, red line in Fig. 3f), and from that calculated τ_o for individual, independently gated IP_3R ($=N\tau_{o,N}$). Both analyses gave the same result: τ_o for IP_3R within a cluster was reduced to 47% of that for lone IP_3R (Fig. 3f). A similar analysis of closed states confirmed that neither was affected by clustering (Supplementary Fig. 5, Supplementary Table 3). IP_3-evoked clustering almost doubles the rate of channel closure ($1/\tau_o$) and this is alone sufficient (Supplementary Fig. 6, Supplementary Table 4) to

account for the decreased P_o of clustered IP_3R (Fig. 2g). Clustered IP_3R open for half as long as lone IP_3R (5.4 *vs* 11.9 ms), and pairing of IP_3R is enough to cause the full effect (Fig. 2g). Other regulators of IP_3R usually influence τ_c and so rates of channel opening4. The difference is important because τ_o will affect the time course of the initial Ca^{2+} release within elementary events7 and thereby Ca^{2+}-mediated interplay between clustered IP_3R. This is confirmed by simulations of intracellular Ca^{2+} spikes, where the ~50% decrease in τ_o of clustered IP_3R causes the frequency of Ca^{2+} spiking to decrease by 4-fold (Supplementary Fig. 7).

Within a patch, cluster size is limited to the number of IP_3R fortuitously caught beneath the patch-pipette, but for nuclei pre-treated with bath-applied IP_3 the clusters are larger (Fig. 3c). This demonstrates that a maximal concentration of IP_3 causes >93% of IP_3R to cluster (85/91 IP_3R from 88 nuclei pre-treated with IP_3) and the average cluster contains 4.25 ± 0.38 IP_3R (Methods). Inhibition of IP_3R within a cluster is not caused by feedback inhibition4 from Ca^{2+} passing through neighbouring IP_3R. Both BS and PS have the same $[Ca^{2+}]$ and are buffered with BAPTA, the inhibition occurs at positive (Fig. 2) and negative holding potentials (Supplementary Discussion), and clustered IP_3R open independently (Fig. 2f). Because permeating ions cannot regulate neighbouring IP_3R under our recording conditions, inhibition must be mediated by contacts between IP_3R. From this, we estimate that the average separation of IP_3R falls from ~1 μm to ~20 nm after clustering, and that clusters are ~2 μm apart (Supplementary Discussion). These spacings concur with confocal measurements suggesting that a Ca^{2+} puff originates from a cluster ~50 nm wide and that clusters are ~3 μm apart18. When expressed at high densities, IP_3R19 and ryanodine receptors20 form arrays with each tetrameric receptor contacting four others. We speculate that IP_3-evoked clusters (of 4.25 ± 0.38 IP_3R) exploit similar contacts and so, with single IP_3R, form the fundamental units of Ca^{2+} signalling (Fig. 3g).

IP_3-evoked clustering is complete within seconds of stimulation with a maximal concentration of IP_3 (Supplementary Fig. 3). To resolve the time course, we used photolysis of caged IP_3 rapidly to increase the IP_3 concentration bathing IP_3R trapped beneath the patch-pipette. IP_3R were initially quiescent and then rapidly activated when IP_3 was photo-released (Fig. 3h). Irrespective of the number of IP_3R caught within a patch, τ_o was initially similar for all IP_3R (~10 ms). It then remained stable for many minutes for lone IP_3R (11.4 ± 0.5 ms), but τ_o fell within 2.5 s to 5.8 ± 0.3 ms for patches containing more than one IP_3R (Fig. 3i, Supplementary Fig. 8). Using τ_o to report IP_3R clustering suggests that clustering is complete within 2.5 s of IP_3 addition. A similar analysis of P_o suggests a half-time for clustering of ~1.5-2 s (Fig. 3i). Our evidence that clustering does not require the cytoskeleton and measurements of IP_3R3 mobility21,22 suggest that diffusion alone may be sufficient to allow IP_3R3 clustering within a few seconds (Supplementary Discussion).

We can define the IP_3 sensitivity of clustering by measuring the extent to which P_o of each IP_3R within a multi-IP_3R patch ($P_o = NP_o/N$, Supplementary Abbreviations) falls below P_o of an identically stimulated lone IP_3R (P_{lone}). This demonstrates that IP_3R clustering (EC_{50} < 300 nM) is ~10-times more sensitive to IP_3 than channel opening (EC_{50} = 2.02 μM, Fig. 3e). Steady-state exposure to low IP_3 concentrations that evoke Ca^{2+} puffs5,7 would, by assembling IP_3R clusters, allow both generation of puffs and loss of Ca^{2+} blips23.

Clustering moves IP_3R (~1 μm apart) from being insulated from their neighbours by Ca^{2+}-buffering to domains (~20 nm apart) where they will instantly experience high local $[Ca^{2+}]$ whenever a neighbour opens24 (Supplementary Fig. 7). Hitherto (Figs 1-3), we prevented such interactions by using K^+ as charge-carrier and recording at a free $[Ca^{2+}]$ (200 nM) that mimics a resting cell. Subsequent experiments include 1 μM free $[Ca^{2+}]$ with IP_3 in PS to simulate the $[Ca^{2+}]$ near open IP_3R. For simplicity we use K^+ as charge-carrier. With 1 μM

[Ca^{2+}] in PS, IP_3R activity was increased: P_o for lone IP_3R almost doubled, as τ_c decreased (Fig. 4a)4. Neither the number of IP_3R/patch (1.12 ± 0.24) nor their random distribution (Fig. 4b) was affected by Ca^{2+}, but the interplay between IP_3R was altered. Whereas clustering reduced the overall activity of IP_3R (NP_o) at resting [Ca^{2+}] (Fig. 2e), the inhibition was reversed by increased [Ca^{2+}], such that the collective activity of a pair of IP_3R (NP_o) was the same as that predicted from the summed activity of two lone IP_3R (Fig. 4c). This did not result from disaggregation of clusters because at increased [Ca^{2+}], IP_3R no longer opened independently. In patches with two IP_3R (open-channel noise prevented analysis of larger clusters), open probabilities did not fit the binomial distribution (Fig. 4e): double open and closed events were over-represented (Supplementary Fig. 9). Furthermore, there were many examples of IP_3R opening and closing directly to and from states with both IP_3R open (Fig. 4d). For paired IP_3R, the double openings were prolonged by 50% (Fig. 4f), but 47% less frequent than expected (Fig. 4g). The overall increase in P_o for double openings was therefore small (12%) and counteracted by a 39% decrease in the probability of only one IP_3R being open and a 116% increase in the probability of both being closed (Fig. 4e). Clustered IP_3R exposed to increased [Ca^{2+}] do not therefore behave independently. Their gating is coupled13,14: they are more likely to open and close together, and their simultaneous openings are prolonged (Supplementary Fig. 9). Coupled gating is not caused by local increases in cytosolic [Ca^{2+}], and must instead result from physical coupling of IP_3R. Under physiological conditions, clustered IP_3R are more likely to experience increased [Ca^{2+}] (because their neighbours may release it), and they are also tuned to respond most to it. By suppressing IP_3R activity at resting [Ca^{2+}], clustering increases the impact of a subsequent local increase in [Ca^{2+}] (Supplementary Fig. 7). Within a cluster, increased Ca^{2+} increases P_o (as it does for lone IP_3R), but it also reverses the inhibition evoked by clustering and it causes coupled gating. These interactions exaggerate the effect of Ca^{2+} within a cluster (Fig. 4h). We conclude that IP_3 dynamically regulates the assembly and behaviour of Ca^{2+} puff sites. IP_3 rapidly drives IP_3R into small clusters, wherein their IP_3 and Ca^{2+} sensitivities are re-tuned to exaggerate Ca^{2+}-mediated recruitment of IP_3R and allow hierarchical recruitment of Ca^{2+} release events (Fig. 4h, Supplementary Fig. 7)5,7.

METHODS SUMMARY

Nuclei from DT40-IP_3R3 cells25 were used for patch-clamp recording from excised patches10.

Supplementary Material

Refer to Web version on PubMed Central for supplementary material.

Acknowledgments

Supported by The Wellcome Trust (CWT), The Biotechnology and Biological Sciences Research Council (CWT), a scholarship from the Jameel Family Trust (TUR), and the IRTG “Genomics and Systems Biology of Molecular Networks” of the Deutsche Forschungsgemeinschaft (MF). We thank S. Dedos for help with DT40 cells, D. Prole and B. Billups for advice, and T. Kurosaki for providing DT40KO cells.

References

1. Berridge MJ, Lipp P, Bootman MD. The versatility and universality of calcium signalling. Nature Rev. Mol. Cell Biol. 2000; 1:11–21. [PubMed: 11413485]
2. Rizzuto R, Pozzan T. Microdomains of intracellular Ca^{2+}: molecular determinants and functional consequences. Physiol. Rev. 2006; 86:369–408. [PubMed: 16371601]

3. Marchant J, Callamaras N, Parker I. Initiation of IP_3-mediated Ca^{2+} waves in Xenopus oocytes. EMBO J. 1999; 18:5285–5299. [PubMed: 10508162]
4. Foskett JK, White C, Cheung KH, Mak DO. Inositol trisphosphate receptor Ca^{2+} release channels. Physiol. Rev. 2007; 87:593–658. [PubMed: 17429043]
5. Bootman MD, Berridge MJ, Lipp P. Cooking with calcium: the recipes for composing global signals from elementary events. Cell. 1997; 91:367–373. [PubMed: 9363945]
6. Horne JH, Meyer T. Elementary calcium-release units induced by inositol trisphosphate. Science. 1997; 276:1690–1694. [PubMed: 9180077]
7. Marchant JS, Parker I. Role of elementary Ca^{2+} puffs in generating repetitive Ca^{2+} oscillations. EMBO J. 2001; 20:65–76. [PubMed: 11226156]
8. Shuai J, Rose HJ, Parker I. The number and spatial distribution of IP_3 receptors underlying calcium puffs in Xenopus oocytes. Biophys. J. 2006; 91:4033–4044. [PubMed: 16980372]
9. Sneyd J, Falcke M. Models of the inositol trisphosphate receptor. Prog. Biophys. Mol. Biol. 2005; 89:207–245. [PubMed: 15950055]
10. Dellis O, Dedos S, Tovey SC, Rahman T-U, Dubel SJ, Taylor CW. Ca^{2+} entry through plasma membrane IP_3 receptors. Science. 2006; 313:229–233. [PubMed: 16840702]
11. Mak D-O,D, Foskett JK. Single-channel kinetics, inactivation, and spatial distribution of inositol trisphosphate (IP_3) receptors in *Xenopus* oocyte nucleus. J. Gen. Physiol. 1997; 109:571–587. [PubMed: 9154905]
12. Ionescu L, Cheung KH, Vais H, Mak DO, White C, Foskett JK. Graded recruitment and inactivation of single $InsP_3$ receptor Ca^{2+}-release channels: implications for quantal Ca^{2+} release. J. Physiol. 2006; 573:645–662. [PubMed: 16644799]
13. Marx SO, Gaburjakova J, Gaburjakova M, Henrikson C, Ondrias K, Marks AR. Coupled gating between cardiac calcium release channels (ryanodine receptors). Circ. Res. 2001; 88:1151–1158. [PubMed: 11397781]
14. Marx SO, Ondrias K, Marks AR. Coupled gating between individual skeletal muscle Ca^{2+} release channels (ryanodine receptors). Science. 1998; 281:818–821. [PubMed: 9694652]
15. Mak D-O,D, Foskett JK. Effects of divalent cations on single-channel conduction properties of *Xenopus* IP_3 receptor. Am. J. Physiol. 1998; 275:C179–C188. [PubMed: 9688849]
16. Tateishi Y, et al. Cluster formation of inositol 1,4,5-trisphosphate receptor requires its transition to open state. J. Biol. Chem. 2005; 280:6816–6822. [PubMed: 15583010]
17. Bourguignon LY, Iida N, Jin H. The involvement of the cytoskeleton in regulating IP_3 receptor-mediated internal Ca^{2+} release in human blood platelets. Cell Biol. Int. 1993; 17:751–758. [PubMed: 8220303]
18. Dargan SL, Parker I. Buffer kinetics shape the spatiotemporal patterns of IP_3-evoked Ca^{2+} signals. J. Physiol. 2003; 553:775–788. [PubMed: 14555715]
19. Katayama E, et al. Native structure and arrangement of inositol-1,4,5-trisphosphate receptor molecules in bovine cerebellar Purkinje cells as studied by quick-freeze deep-etch electron microscopy. EMBO J. 1996; 15:4844–4851. [PubMed: 8890158]
20. Yin CC, Blayney LM, Lai FA. Physical coupling between ryanodine receptor-calcium release channels. J. Mol. Biol. 2005; 349:538–546. [PubMed: 15878596]
21. Fukatsu K, Bannai H, Zhang S, Nakamura H, Inoue T, Mikoshiba K. Lateral diffusion of inositol 1,4,5-trisphosphate receptor type 1 is regulated by actin filaments and 4.1N in neuronal dendrites. J. Biol. Chem. 2004; 279:48976–48982. [PubMed: 15364918]
22. Ferreri-Jacobia M, Mak D-O,D, Foskett JK. Translational mobility of the type 3 inositol 1,4,5-trisphosphate receptor Ca^{2+} release channel in endoplasmic reticulum membrane. J. Biol. Chem. 2005; 280:3824–3831. [PubMed: 15537642]
23. Sun X-P, Callamaras N, Marchant JS, Parker I. A continuum of $InsP_3$-mediated elementary Ca^{2+} signalling events in *Xenopus* oocytes. J. Physiol. 1998; 509:67–80. [PubMed: 9547382]
24. Falcke M. Reading patterns in living cells - the physics of Ca^{2+} signaling. Adv. Phys. 2004; 53:255–440.

25. Boehning D, Joseph SK, Mak D-O,D, Foskett JK. Single-channel recordings of recombinant inositol trisphosphate receptors in mammalian nuclear envelope. Biophys. J. 2001; 81:117–124. [PubMed: 11423400]

26. Prole DL, Lima PA, Marrion NV. Mechanisms underlying modulation of neuronal KCNQ2/KCNQ3 potassium channels by extracellular protons. J. Gen. Physiol. 2003; 122:775–793. [PubMed: 14638935]

Europe PMC Funders Author Manuscripts

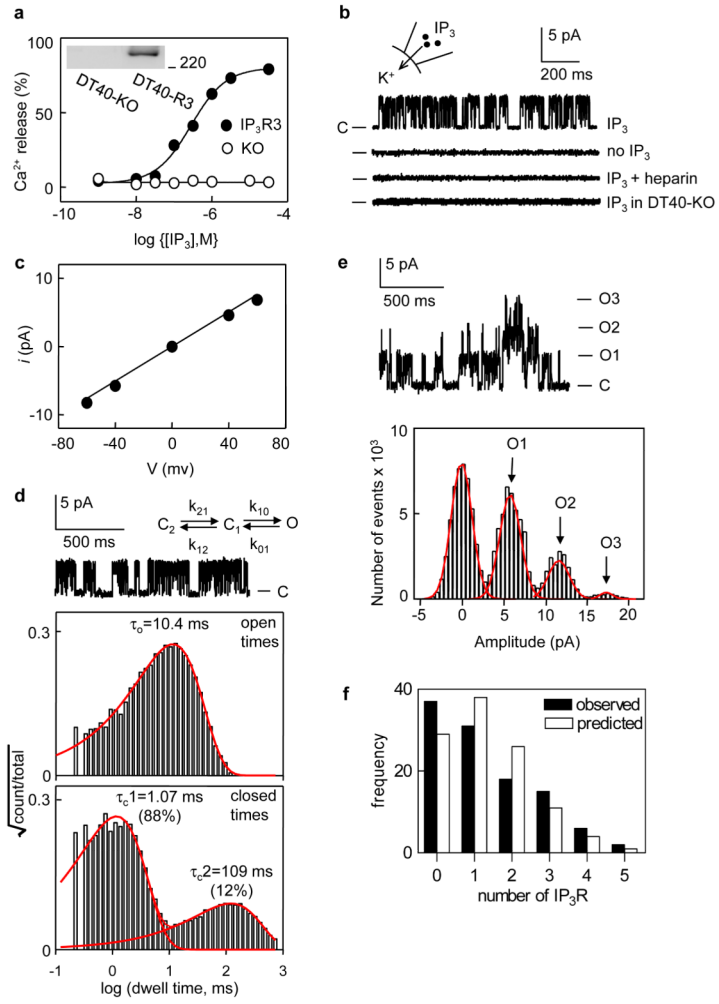

Figure 1. IP_3R are randomly distributed

a, IP_3-evoked Ca^{2+} release from permeabilized DT40-IP_3R3 (EC_{50} = 281 ± 46 nM) and DT40-KO cells (means ± SEM, n ≥ 3). Immunoblot with IP_3R3-specific antiserum (10 μg membrane protein/lane, 220-kDa marker shown). **b**, Currents recorded from excised patches with 10 μM IP_3 in PS. No currents were detected without IP_3 (n = 20), with heparin (100 μg/ml) and IP_3 (n = 15), or with IP_3 in DT40-KO cells (n > 30). C denotes closed state. **c**, *i*-V relationship for IP_3-evoked current (γ_K = 121 ± 2.8 pS, n = 7). **d**, Dwell time distribution of single IP_3R3 stimulated with 10 μM IP_3. Open time distribution of this typical recording is fitted with a single probability density function (pdf) with τ_o = 10.4 ms (mean = 11.9 ± 1.6 ms, n = 6). The pdf for the τ_c distribution has two components (1.07 ms, 88% and 109 ms, 12%). Dwell time distributions are consistent with the gating scheme (Supplementary Methods, Supplementary Figs 5, 6). **e**, Typical all-points current amplitude histogram of an excised patch containing 3 IP_3R stimulated with 10 μM IP_3; C and O denote closed and open states. **f**, Observed and predicted numbers of IP_3R/patch from 109 patches (mean = 1.34) stimulated with 10-100 μM IP_3.

Europe PMC Funders Author Manuscripts

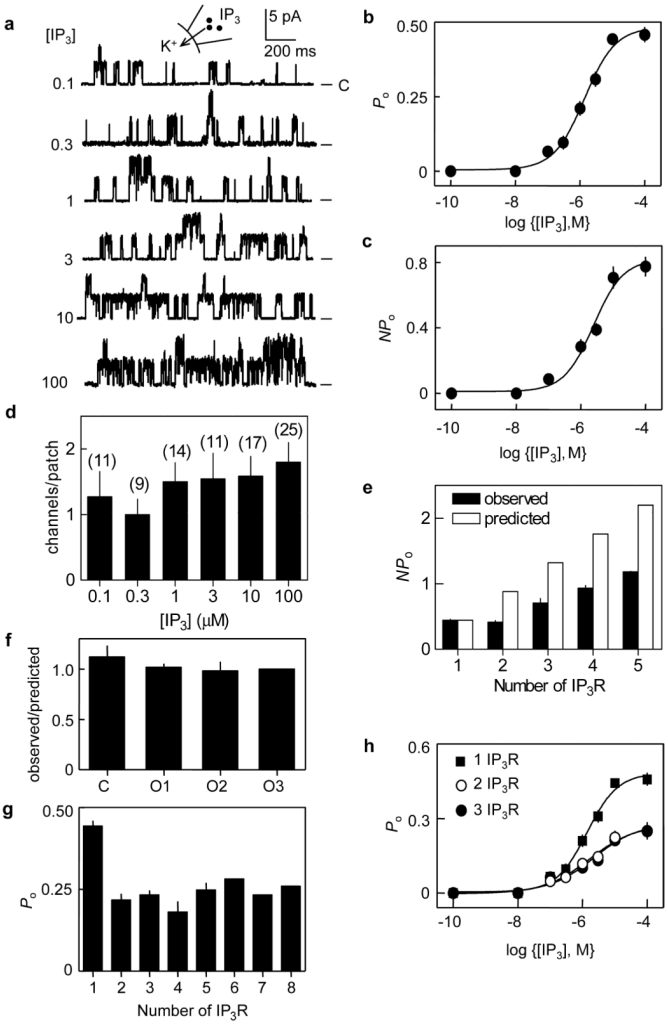

Figure 2. Lone IP_3R are more active than clustered IP_3R at resting cytosolic Ca^{2+}

a, Typical records from patches (2 IP_3R/patch) stimulated with IP_3 (μM). **b**, **c**, Effect of IP_3 on P_o of patches containing a single IP_3R (b) or on NP_o of patches with 3 IP_3R (c) (n ≥ 4). **d**, Numbers of IP_3R detected in each patch for each IP_3 concentration (n = 9-25). **e**, Predicted (ie NP_{lone}) and observed NP_o for patches containing 1-5 IP_3R (n ≥ 3; n = 2 for 5-IP_3R patch). **f**, For patches with 3 IP_3R, observed/predicted values are shown for the indicated numbers of simultaneous openings (Supplementary equation 4). **g**, P_o as a function of the number of IP_3R within a patch after stimulation with 10 μM IP_3 (Supplementary equation 5). **h**, Effect of IP_3 on P_o for lone IP_3R and IP_3R within multi-IP_3R patches (n ≥ 4).

Europe PMC Funders Author Manuscripts

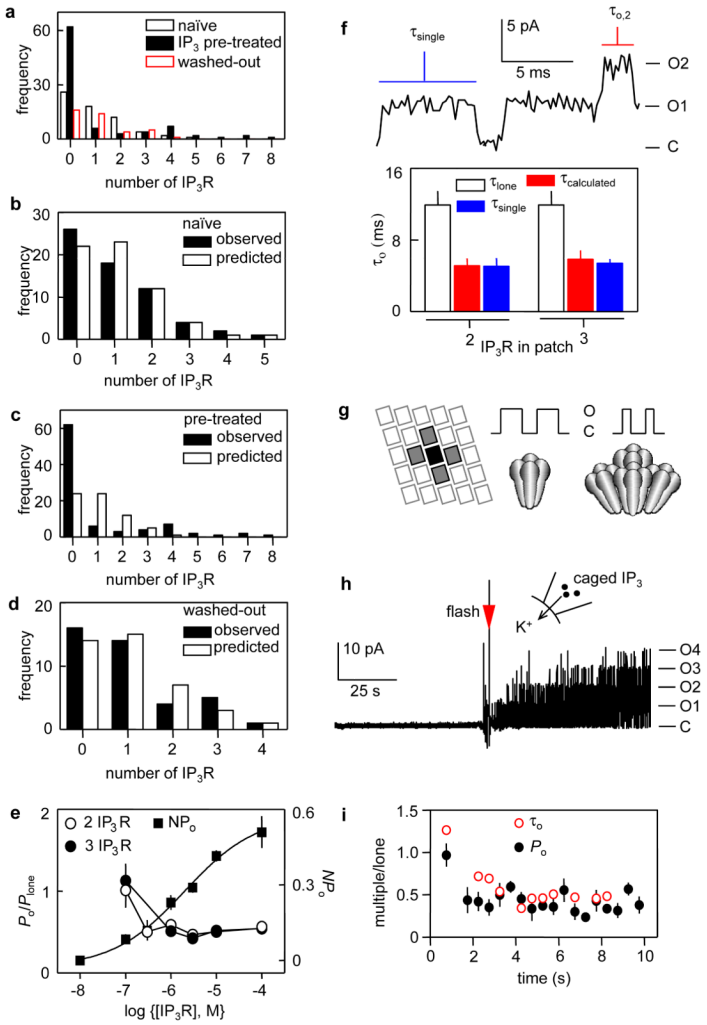

Figure 3. Reversible clustering of IP_3R by IP_3

a, Numbers of IP_3R detected in patches from naive nuclei (n = 63), after pre-treatment with bath-applied IP_3 (10 μM, ~2 min; n = 88), or the latter after recovery for 8-10 min without IP_3 (n = 40). **b-d**, Observed and predicted numbers of IP_3R/patch. **e**, Effects of IP_3 on IP_3R clustering and gating. Clustering is reported by P_o/P_{lone} for patches with 2 or 3 IP_3R, and gating by NP_o for patches with 2 IP_3R (EC_{50} = 2.02 ± 0.20 μM). **f**, τ_o for patches with 2 or 3 IP_3R measured from the duration of single channel openings (blue line, τ_{single}) or calculated from the duration of openings to the N^{th} level (red line, $\tau_{calculated} = N.\tau_{o,N}$). These are compared with τ_o for lone IP_3R (τ_{lone}). Typical trace is from a patch with 2 IP_3R. **g**, IP_3 drives IP_3R into small clusters consistent with arrays (grey) formed by IP_3R at high density19. Within a cluster, each IP_3R opens independently, but closes more rapidly than a lone IP_3R. **h**, Typical recording from a patch containing 4 IP_3R with IP_3 released from caged IP_3 in PS by flash photolysis (electrical noise caused by the flash is shown). **i**, From records similar to h (Supplementary Fig. 8), P_o (from NP_o/N) and τ_o were measured during each 0.5 s interval after the flash (1.5 s for first interval). The ratio (multi-IP_3R patch/lone IP_3R) is shown for both τ_o and P_o. Results (means ± SEM) are from 4 (single) and 7 (multiple, with 2-4 IP_3R/patch) patches.

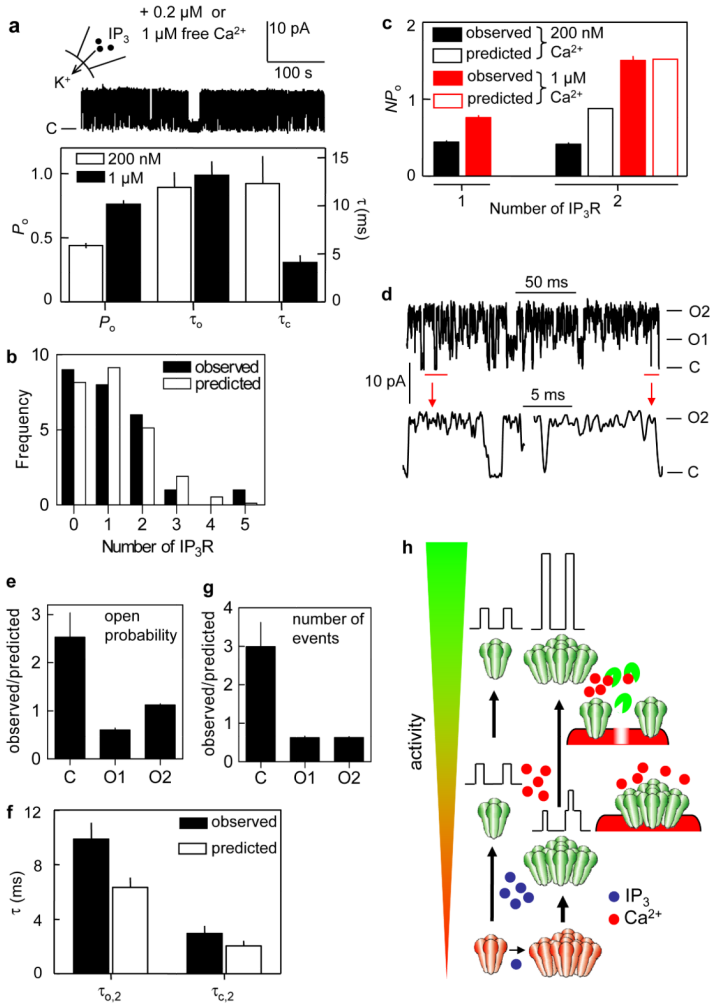

Figure 4. Clustering retunes Ca^{2+} regulation of IP_3R

a-e, Patches were stimulated with PS containing 10 μM IP_3 and (unless otherwise stated) 1 μM Ca^{2+}. **a**, Typical recording and summary data (n = 5-6) from lone IP_3R show that increasing Ca^{2+} increases P_o by reducing τ_c. **b**, Observed and expected numbers of IP_3R/patch. **c**, Observed and predicted NP_o for patches containing 1 or 2 IP_3R and stimulated with 10 μM IP_3 in PS containing 200 nM or 1 μM Ca^{2+} (n = 5-6). **d**, Typical recording from a patch with 2 IP_3R, enlarged (red) to highlight transitions directly between closed (C) and double open (O2) states. **e**, Observed and predicted P_o for closed (C) and single (O1) or double openings (O2) for patches with 2 IP_3R (n = 6, Supplementary equations 4, 5). **f**, Observed and expected durations of events when both IP_3R are simultaneously open ($\tau_{o,2}$) or closed ($\tau_{c,2}$) for patches with 2 IP_3R (n = 6, Supplementary equations 6, 7). **g**, Observed and predicted numbers of transitions to each of the 3 states in a patch with 2 IP_3R (n = 6)26. **h**, At resting [Ca^{2+}], IP_3 drives IP_3R into small clusters wherein IP_3R gate independently, but with reduced P_o and IP_3 sensitivity. Ca^{2+} reverses the inhibition imposed by clustering, openings within a cluster are more synchronized, and simultaneous openings are prolonged. Clustering primes IP_3R to respond by repressing their activity, and then allowing Ca^{2+} to unleash the coordinated gating of clustered IP_3R (Supplementary Fig. 7).

Europe PMC Funders Author Manuscripts